The Journal of Experimental Biology 215, 605-616

doi:10.1242/jeb.063578

## RESEARCH ARTICLE

# Effect of particulate contamination on adhesive ability and repellence in two species of ant (Hymenoptera; Formicidae)

Matthew J. Anyon[1,2,*,†], Michael J. Orchard[3,†], David M. A. Buzza[1,2], Stuart Humphries[3] and Mika M. Kohonen[2,‡]

[1]Department of Physics, [2]Surfactant & Colloid Group, Department of Chemistry and [3]Functional Ecology Group, Department of Biological Sciences, University of Hull, Hull HU6 7RX, UK

*Author for correspondence (m.j.anyon@2005.hull.ac.uk)
†These authors contributed equally to this work
‡Present address: Department of Quantum Science, Australian National University, ACT 0200, Canberra, Australia

Accepted 1 November 2011

**SUMMARY**

**Tarsal adhesive pads are crucial for the ability of insects to traverse their natural environment. Previous studies have demonstrated that for both hairy and smooth adhesive pads, significant reduction in adhesion can occur because of contamination of these pads by wax crystals present on plant surfaces or synthetic microspheres. In this paper, we focus on the smooth adhesive pads of ants and study systematically how particulate contamination and the subsequent loss of adhesion depends on particle size, particle surface energy, humidity and species size. To this end, workers of ant species *Polyrhachis dives* and *Myrmica scabrinodis* (Hymenoptera; Formicidae) were presented with loose synthetic powder barriers with a range of powder diameters (1–500 μm) and surface energies (PTFE or glass), which they would have to cross in order to escape the experimental arena. The barrier experiments were conducted for a range of humidities (10–70%). Experimental results and scanning electron microscopy confirm that particulate powders adversely affect the adhesive ability of both species of ant on smooth substrates *via* contamination of the arolia. Specifically, the loss of adhesion was found to depend strongly on particle diameter, but only weakly on particle type, with the greatest loss occurring for particle diameters smaller than the claw dimensions of each species, and no effect of humidity was found. We also observed that ants were repelled by the powder barriers which led to a decrease of adhesion prior to their eventual crossing, suggesting that insect antennae may play a role in probing the mechanical fragility of substrates before crossing them.**

Key words: arolium, contamination, Hymenoptera, particles, powder barrier, wet adhesion.

## INTRODUCTION

Insects have evolved numerous adaptations to enable them to move rapidly across natural surfaces within their ecological niches. Efficient adhesion is crucial for many different aspects of an insect's life, such as mating and oviposition (Bitar et al., 2009; Bitar et al., 2010), foraging and prey capture (Hölldobler and Wilson, 1990; Bauer et al., 2008), defence (Eisner and Aneshansley, 2000; Betz and Kolsch, 2004) and the selection and construction of nesting sites (Federle et al., 1997), especially for arboreal insects (Federle et al., 2002).

When surfaces are rough, insects can utilise their tarsal claws to attach to surface asperities (Federle et al., 2002). However, adhesion to smooth substrates is facilitated by special adhesive pads that have convergently evolved several times to conform to one of two main types: 'hairy' (arrays of microscopic setae) and 'smooth' (soft deformable pads) (Gorb and Beutel, 2001). It has been found that both pad types in insects deposit a liquid secretion to the contact zone during locomotion, with adhesion mediated by capillary and viscous attractive forces acting during static and dynamic situations, respectively (Nachtigall, 1974; Stork, 1980a; Walker et al., 1985; Ishii, 1987; Wigglesworth, 1987; Lees and Hardie, 1988; Dixon et al., 1990; Walker, 1993; Gorb, 1998; Federle et al., 2002). Adhesion has been found to be strongly related to the contact area of the attachment pads with the substrate, thus presence of the liquid aids adhesion by maximising the contact area between the pad and substrate by filling in micro-surface asperities (Vötsch et al., 2002; Drechsler and Federle, 2006; Dirks et al., 2009).

Many climbing insects (e.g. ants and beetles) spend much time walking on plant surfaces and require strong adhesion when walking vertically or upside down, sometimes carrying the equivalent of several times their own body weight (Hölldobler and Wilson, 1990). As such, it is necessary to continually ensure the effective functioning of their adhesive devices. However, it has been observed that many plants possessing fragile waxy layers or crystals are able to provide effective barriers against climbing insects (Stork, 1980b; Federle et al., 1997; Federle et al., 2000; Markstädter et al., 2000; Gorb and Gorb, 2002; Eigenbrode, 2004; Gaume et al., 2004; Gorb et al., 2008; Borodich et al., 2010). It has been proposed (Gorb and Gorb, 2002) that this anti-adhesive effect arises from the fact that the wax crystals are easily detached from the plant cuticle, breaking off when insects walk on them, contaminating the insects' attachment devices. Contamination of attachment pads drastically reduces the contact area between the pad and the substrate, reducing overall adhesive forces. Substrate properties such as the surface energy and surface topography of these wax particles can influence the adhesive forces in insects, and a combination of these influences has been shown to drastically reduce the adhesive ability of beetles such as *Gastrophysa viridula* (Coleoptera; Chrysomelidae), which

possess hairy adhesive pads (Gorb and Gorb, 2009). Similar effects have also been found for synthetic powder barriers, which have been found to form effective barriers against crawling insects (Briscoe, 1943; Alexander et al., 1944; Merton, 1956; Boiteau et al., 1994; Glenn et al., 1999); such barriers could potentially be used as an ecologically friendly method for the control of insect pest species (Boiteau et al., 1994; Hunt and Vernon, 2001). However, there have been few studies of how the anti-adhesive properties of natural or synthetic particle barriers depend on the physicochemical properties of the contaminating particles. In this paper, we focus on the smooth adhesive pads of ants and study systematically how particulate contamination by synthetic powder barriers and the subsequent loss of adhesion depends on particle size, particle surface energy and humidity.

Insects are able to reduce the detrimental effects of attachment pad contamination by using a number of different strategies that can be categorised under (1) passive 'self-cleaning' mechanisms, which have been found in insects with both smooth and hairy pad types (Clemente et al., 2010; Orchard et al., 2012), as well as geckos (Hansen and Autumn, 2005; Lee and Fearing, 2008); and (2) active grooming behaviours (see Hosoda and Gorb, 2011). In particular, Clemente et al. have found that both smooth and hairy pads exhibit self-cleaning properties when contaminated with glass microspheres in a range of sizes (1–45 μm), finding that adhesion forces can return to normal after several steps (Clemente et al., 2010). Specifically for smooth adhesive pads, they found that self-cleaning was aided by shear movement of the tarsal pads in the proximal direction. Reduction of adhesive force has also been found to trigger grooming behaviour in beetles walking on manufactured nanostructured surfaces (Hosoda and Gorb, 2011), demonstrating that the reduction of adhesion or friction force between tarsal attachment pads and the substrate provides the insect with information on the amount of contamination of its adhesive pad, influencing their behaviour.

However, although grooming behaviours can remove particles from already contaminated attachment pads, to prevent contamination from initially occurring in the first place, it is reasonable to assume that insects may possess a system of detection and avoidance *via* their antennae. Specifically, it is possible that insects may also be able to use their antennae to 'detect' the material properties, such as surface morphology and roughness, of a substrate – in this case a powder barrier. Indeed, it is documented that insects use their antennae to detect numerous aspects of their surroundings (Kevan and Lane, 1985; Crook et al., 2008), with recent work demonstrating that the information relayed from tactile influences (Bernadou and Fourcassie, 2008; Bernadou et al., 2009) can be used in decision-making (Camhi and Johnson, 1999). However, this important question has yet to be addressed in a systematic way for loose powder barriers. Thus the second aim of this paper is to determine to what extent the ant species used are repelled by the powder barriers and how this behaviour may also be influenced by the physicochemical nature of the powder barrier. In order to study the effect of powder barriers on insect adhesion and repellence, worker ants from the species *Polyrhachis dives* Smith 1857 and *Myrmica scabrinodis* Nylander 1846 (Hymenoptera; Formicidae) were placed within the centre of circular barriers constructed of loose powders of synthetic particles, and their behaviour and adhesive ability after crossing the barrier was observed. These species are representative of the insect order Hymenoptera, both possessing smooth adhesive pads known as arolia (Gladun et al., 2009). These species were chosen in order to compare the behaviour and subsequent attachment ability of species of contrasting size and which are native to different ecological niches. Firstly, the insects' ability to climb vertical smooth surfaces after traversing the barriers was tracked. Secondly, the time spent investigating the barriers themselves with their antennae, a behaviour known as 'antennating' (Bernadou and Fourcassie, 2008), before the insect attempted to cross was recorded. During all experiments, the effects of the powder particles on attachment ability were investigated systematically by changing the particle material and size, and the relative humidity at which the experiments were performed, to elucidate the factors affecting insect adhesion and repellence.

## MATERIALS AND METHODS

### Insects

Worker ants were extracted from colonies of *P. dives* and *M. scabrinodis* purchased from a supplier (Anstore, Berlin, Germany). Colonies were held in glass formicaria in the laboratory and maintained at 20–25°C under a 14 h:10 h light:dark cycle. Each species was fed an ant-feed mixture (Antstore), dried seeds and dried insects *ad libitum* several times a week.

The length of the insects' claws and claw basal distance – defined here as the distance between the claws at the point at which they emerge from the tarsal cuticle – were measured by imaging the tarsi with a digital camera (Canon Powershot S31S, Canon UK Ltd, Reigate, Surrey, UK) connected to a Nikon SMZ800 stereo-optical microscope (Jencons-PLS, East Grinstead, West Sussex, UK) *via* an adaptor mount (MM99 S/N 3506, Martin Microscope Co., Easley, SC, USA). Digital images were analysed using the software package ImageJ (ImageJ 1.40, National Institutes of Health, Bethesda, MD, USA) (Rasband, 1997–2009). Visualisation of contamination of the insect tarsi and antennae was achieved using scanning electron microscopy (SEM). Insect samples were air-dried, coated with 2 nm of gold-palladium and imaged using a Zeiss EVO60 electron microscope in high-vacuum mode at 2 kV beam voltage and 100 pA probe current.

### Powder particles

Polytetrafluoroethylene (PTFE; Sigma-Aldrich, Dorset, UK) and soda lime Ballotini glass (VWR-Jencons, Lutterworth, Leicestershire, UK) particles of various diameters, along with 1 μm diameter silica-glass (Angström Spheres, Fibre Optic Centre Inc., New Bedford, MA, USA), were used in this study. The PTFE and glass particles are representative of particles with low and high surface energy, respectively. Particles were separated into well-defined size fractions by manual agitation through a series of Endecott powder sieves (UKGE Ltd, Southwold, Suffolk, UK) of decreasing grating diameter between 500 and 10 μm. The geometry and morphology of the two materials differed, with glass particles shaped as regular spheres, in contrast to the PTFE particles, which were irregularly shaped and rough (Fig. 1). Diameters reported for the PTFE particles were determined from the mean value of the major and minor length axes, which led to a small variation in the mean values of each fraction between materials, as reported in Table 1. Using light microscopy and SEM images, the physical size distributions of the particles within each fraction were determined using an in-built macro in ImageJ that counts and determines the size of objects within the image (Table 1).

### Barrier experiments

Circular powder barriers of ~1 cm width were constructed inside open glass Petri dishes of radius $r$=6.4 cm and $r$=3.3 cm for *P. dives* and *M. scabrinodis*, respectively ($h_{dish} >> h_{ant}$, where $h$ is the height). Particles from each of the size fractions were gently poured

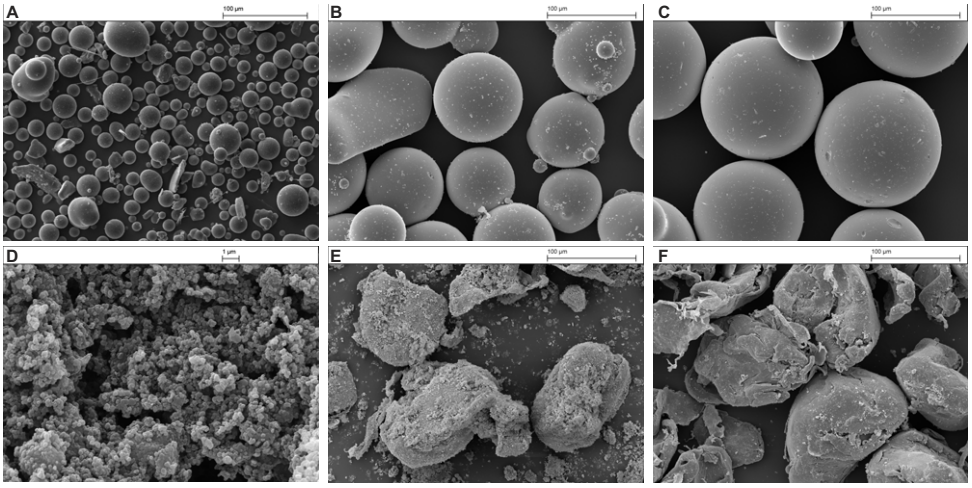


Fig. 1. Scanning electron microscopy (SEM) images of some representative powder fractions of (A–C) glass and (D–F) polytetrafluoroethylene (PTFE) particles used to construct the loose powder barriers. Glass particles are shaped as regular spheres, in contrast to the PTFE particles, which are irregularly shaped. The mean sizes of the particles are reported above in Table 1. Scale bars, 100 μm in all panels except D (1 μm).

manually along the inside wall of the dish using a small Teflon funnel. Prior to construction, Petri dishes were rinsed with HPLC grade iso-propanol (Fisher Scientific UK, Ltd, Loughborough, UK), wiped with a clean-room Spec-Wipe (VWR-Jencons) and dried with a filtered air supply. A fresh barrier was constructed for each replicate to reduce any effects of chemical signalling between workers from one experiment to the next. To neutralize any static charges, an ion gun (Zerostat 3, Milty, Bishops Stortford, UK) was used on each barrier before the experiments were begun. Petri dishes containing the barriers were placed upon an Ecotherm heat/cold stage (Torrey Pines Scientific Inc., Carlsbad, CA, USA) within a custom-built Perspex chamber to allow for temperature control within the experimental arena (Fig. 2). An air supply was passed through a series of moisture (R&D Separations MT200-4, Krackeler Scientific, Inc., Albany, NY, USA) and hydrocarbon traps (Agilent HT200-4, Agilent Technologies, Edinburgh, UK), which allowed control of the relative humidity (RH) of the airflow linked to the chamber. RH was monitored using a HIH-4000-001 Integrated Circuitry Humidity Sensor (Honeywell Sensing and Control, Golden Valley, MN, USA) and logged with a Picoscope 3224 PC-based oscilloscope (Pico Technology Ltd, St Neots, UK). In order to study the effect of humidity on the number of ants to escape from a given fraction, the initial barrier experiments were carried out at 10, 50 and 70% RH (±5%) at a fixed temperature of 25±2°C. This range was chosen as it represented the natural range of RH each ant species was likely to encounter in their ecological niches or natural habitats when traversing dry surfaces (Hölldobler and Wilson, 1990). Finally, to avoid any moisture-induced improvement of adhesion between insect species and powder fractions during the experiments, all insects were held within closed dishes at the same RH for at least 30 min prior to use (Voigt et al., 2010). Control experiments were performed at each humidity level using clean dishes with no powders.

Table 1. Measured diameters (±s.d.) of the polytetrafluoroethylene (PTFE) and glass particles after sieving into different sized fractions

| Material | Mean diameter (μm) |
|---|---|
| PTFE | 476±72 |
| PTFE | 123±60 |
| PTFE | 105±76 |
| PTFE | 21±23* |
| Glass | 141±25 |
| Glass | 111±24 |
| Glass | 19±8 |
| Glass | 1±0.1* |

Particle sizes were determined using optical and scanning electron micrograph images; typical sample size was ~150 particles. The 1 μm diameter glass particles had a standard deviation of <10% as defined by the supplier.
*Particles were used as supplied and were not sieved.

Workers were carefully extracted from their colonies and placed into the centre of the Petri dish, using soft metal tweezers, *via* a small access hole on the top surface of the chamber (Fig. 2). Ants were observed for a maximum of 5 min, or until the ant had escaped, with each ant used only once and between 30 and 40 replicates performed for each parameter combination (*M. scabrinodis* $N_{total}$=264, *P. dives* $N_{total}$=277). Experiments were filmed from above using a digital camera (QuickCam Pro for Notebooks, Logitech UK Ltd, Slough, UK) controlled by HandyAVI 4.3 (Azcendant, Tempe, AZ, USA) using the time-lapse capture mode, in a manner similar to that detailed by Loeffler (Loeffler, 2009).

Two parameters were measured. The first was the number of ants that were trapped inside the arena by the powders. Specifically, the results of each barrier experiment had three classifications: escape – the ant successfully escaped from the arena within 5 min; trapped – the insect attempted but failed to escape within 5 min; and no attempt – the insect made no attempt to cross the barrier and escape from the arena within 5 min. Denoting the number of ants that escaped, were trapped or made no attempt to cross the barriers as $N_e$, $N_t$ and $N_n$, respectively, the percentage of ants trapped for each parameter combination was defined as:

$$\%\text{Trapped} = \frac{N_t}{N_t + N_e} \times 100 \ . \quad (1)$$

Although $N_n$ needed to be taken into account, it was excluded from our analyses as these outcomes could not be attributed to any effects of contamination by the barriers.

Second, to determine to what extent the powders repelled the ants, the activity of each worker was recorded throughout the experiments and the length of time between the start of the experiment and the ant's first attempt to cross powder barrier threshold, $T_r$, was measured.

To investigate the effect barrier fragility has on the measured parameters, 19 μm diameter glass particles were also used to construct a series of solid, or 'caked', barriers for comparison. The caked barriers were prepared by constructing loose barriers, in the same manner as described above, which were then covered with a

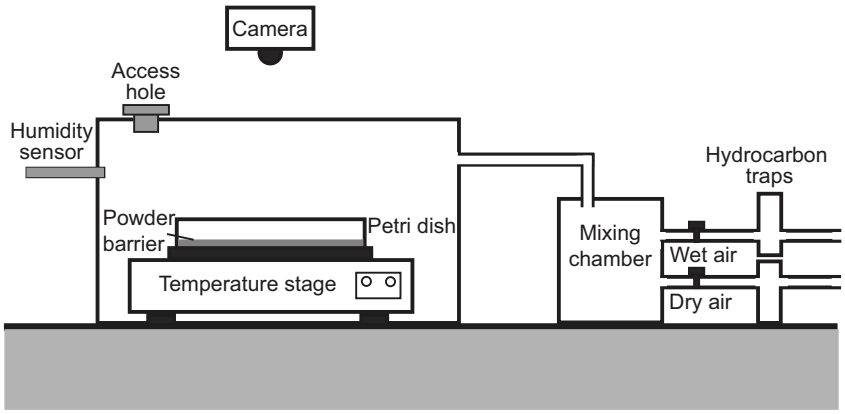


Fig. 2. Schematic of the apparatus for the barrier experiments. The glass Petri dish sits on a heat/cold stage, which maintains the temperature within the arena for the duration of the experiment. The insects are carefully introduced to the centre of the Petri dish *via* an access hole at the top using soft tweezers and are filmed from above for 5 min.

non-airtight plastic lid to protect them from any dust particles, and left exposed to the atmosphere for at least 24 h (30–40% RH). Glass particles, such as those used in this study, form weak siloxane bonds at humidities greater than 30% at the contact points of the particles because of the amount of water vapour present in the atmosphere, which leads to a slow solidification of the barrier (Bocquet et al., 1998; Fraysse et al., 1999; Bocquet et al., 2002). These barriers were sturdy enough to remain intact when the dish was inverted, but could be easily broken apart by manual pressure. This effect does not occur for PTFE particles, so this experiment could only be performed using high surface energy particles. All caked barrier replicates were performed under laboratory atmosphere (25±5°C, 35±5% RH) with the same procedure as above, and were filmed for a maximum of 10 min. During all experiments, no individual insect was used twice in any 24 h period. Statistical analyses were performed using R v.2.8.1 (R Core Development Team, 2010). Escape data were analysed using a linear model with binomial distribution, and time repelled ($T_r$) and time to escape ($T_e$) were analysed with either an ANOVA for parametric data or a linear model for non-parametric data.

## RESULTS

### Insects

Individual workers were weighed and their claw length and basal distance were measured from optical and SEM images to allow for comparison of the two species (Table 2).

### Loose powder barriers

#### Trapping of ants

Control experiments with clean dishes trapped no ants of either species for all humidities investigated. Within the measured range of humidities, when subject to Kaplan–Meir survival analysis, the effect of RH on the percentage of ants trapped by any loose barriers was not significant for either species ($\chi^2$=3.52, d.f.=2, $P$>0.05), thus replicates from experiments across different RH values were subsequently pooled for further analyses.

The percentage of ants trapped, as defined by Eqn 1, was determined for each particle fraction (Fig. 3). For both *P. dives* and *M. scabrinodis*, the percentage of ants trapped was found to be inversely related to the particle diameter for both materials, with smaller particles of both PTFE and glass trapping a significantly greater number of individuals (*P. dives*: glass, $F_{3,134}$=92.96, $P$<0.001; PTFE, $F_{3,135}$=50.75, $P$<0.001; *M. scabrinodis*: glass, $F_{3,135}$=41.037, $P$<0.001; PTFE, $F_{3,121}$=15.04, $P$<0.001). Within each species of ant, particle size was found to have a significant effect on the percentage of ants trapped, with smaller particles trapping a larger percentage of ants compared with larger particles (ANOVA: *P. dives*, $F_{7,223}$=48.70, $P$<0.001; *M. scabrinodis*, $F_{7,270}$=20.12, $P$<0.001). A similar result was found when comparing percentage of ants trapped between the two species, indicating that the relationship between contamination and particle size is similar for both species (ANOVA: $F_{7,501}$=10.11, $P$<0.001).

Several *P. dives* workers that had traversed the different barriers, but were manually prevented from attempting to climb the vertical glass wall, were killed immediately after they had crossed the barrier and their tarsi were imaged *via* SEM (Fig. 4B–H); as a control, we also show the uncontaminated tarsi of *P. dives* (Fig. 4A). Contamination of the arolia by particles was observed for both PTFE and glass barriers made from small particles. Specifically, the arolia along with the tarsal claws and portions of the most distal tarsal segment were heavily contaminated by small particles (Fig. 4B–D) and the amount of particles observed to remain adhered to the tarsus and arolium increased with decreasing particle diameter for both materials. Indeed, the 1 μm glass particles almost completely coated the distal segment of the tarsi.

When comparing between *P. dives* and *M. scabrinodis*, the percentage of ants trapped by glass or PTFE powders did not differ significantly (ANOVA: $F_{1,513}$=0.8802, $P$>0.05); however, after closer examination it was found that when compared within a species there was a significant effect of particle type on the percentage of ants trapped (*P. dives*, $F_{1,277}$=8.88, $P$<0.05; *M. scabrinodis*, $F_{1,278}$=4.56, $P$<0.05). Specifically, we note that a significantly greater number of *P. dives* workers escaped from within the 19 μm glass barriers compared with the 21 μm PTFE barriers, even though the tarsi of the ants are clearly contaminated in both cases (Fig. 4). This difference was found to be present and significant for both

Table 2. Summary of characteristic measurements made of the two ant species used during this study

| Species | Mass (±s.e.m.; mg) | Claw length (±s.d.; μm) | Claw base distance (±s.d.; μm) |
|---|---|---|---|
| *Myrmica scabrinodis* | 4.83±0.16 | 64±7 | 34.7±6.2 |
| *Polyrhachis dives* | 5.97±0.21 | 110±10 | 123.0±26.2 |

Measurements were taken of multiple individuals of each species ($N$=10).

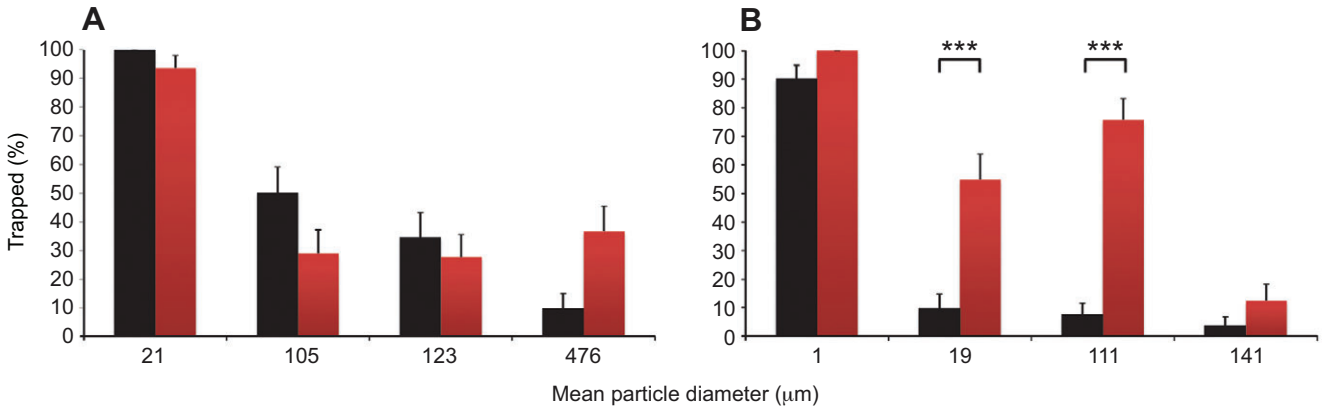


Fig. 3. Percentage of ants trapped as a function of particle size for both (A) hydrophobic PTFE and (B) hydrophilic glass powder barriers. The percentage of *Polyrhachis dives* (black bars) and *Myrmica scabrinodis* (red bars) workers trapped is inversely correlated to particle size for both species (ANOVA, $F_7$=43.982, $P$<0.001). ***$P$<0.001; all others not significantly different between species. Error bars show s.e.m.

species (*P. dives*, $F_1$=48.702, $P$<0.001; *M. scabrinodis*, $F_1$=20.122, $P$<0.01; see Fig. 3).

### Repellent effects of barriers

Ants were observed to investigate several sections of the barriers with their antennae before crossing. Having touched the barriers, ants often spent time grooming their antennae and tarsi. In order to quantify the degree to which the ants were repelled by a powder barrier, the time taken before attempting to cross, $T_r$, was measured for each species–material combination (Fig. 5). It should be noted that although this measurement was used as an indication of the repellence of the barriers, it is only a qualitative estimate because, as mentioned above, a number of ants spent some of their time within the experimental arena grooming themselves. To attain a more accurate measure of actual time spent antennating before crossing the barriers, any time spent cleaning could be measured and subtracted from $T_r$; this could be the subject for a future study. A statistical difference was found when analysing $T_r$ as a function of particle diameter for both species (ANOVA: *P. dives*, $F_{7,225}$=14.41, $P$<0.001; *M. scabrinodis*, $F_{7,272}$=20.21, $P$<0.001). Time repelled data shown in Fig. 5 indicate that for PTFE, $T_r$ is inversely related to particle size for both species of ant, with ants presented with larger particles taking a significantly shorter time to cross the barriers (Fig 5A,C). For glass particles, values of $T_r$ for 19 μm diameter particles were significantly greater than those for all other particle diameters (Fig. 5B,D). There was no significant difference between time measured for the particle types for *M. scabrinodis* (ANOVA: $F_{1,262}$=2.12, $P$>0.05); however, a significant difference was found for *P. dives* (ANOVA: $F_{1,275}$=15.92, $P$=0.03), indicating that, for this ant species, time taken to cross the barriers differed between glass and PTFE.

To ascertain the reason for the lack of antennating behaviour observed by ants for the 1 μm powder barriers, SEM images of the antennae of both ants were taken after workers had crossed barriers constructed of these particles. SEM micrographs of *P. dives* and *M. scabrinodis* antennae show hairs facing in the distal direction, the shafts of which are separated by approximately 5–10 μm. After crossing the 1 μm glass powders, the antennae of both species of ants show a coating of particles in between the hairs (Fig. 6).

To determine the role antennae have on the time repelled, $T_r$, a series of barrier experiments using 19 μm glass powders was carried out using ants with and without their antennae (Fig. 7). A significant difference was found for both species when comparing $T_r$ between individuals with and without antennae: ants without their antennae spent a significantly shorter length of time investigating the barriers before crossing compared with ants with their antennae intact (ANOVA: *P. dives*, $F_{1,62}$=17.93, $P$<0.001; *M. scabrinodis*, $F_{1,61}$=31.538, $P$<0.001).

### Rigid powder barriers

To determine whether the anti-adhesive effect and the observed repellence of the powder barriers is caused by their particulate nature and mechanical fragility, a series of caked powder barriers were constructed with 19 μm glass particles and escape experiments with both caked and fragile barriers were repeated. When comparing between caked and fragile barriers, the percentage of ants trapped as a function of barrier fragility for *M. scabrinodis* was found to be statistically significant ($F_{1,78}$=102.6, $P$<0.001). Specifically, only 7.5% of *M. scabrinodis* remained inside the arena at the end of the experiment with caked barriers compared with 82.5% for the loose barriers (Fig. 8), whereas for *P. dives* there was no significant effect of barrier fragility on percentage of individuals trapped ($F_{1,64}$=1.0, $P$=0.3), with all individuals escaping within the time limit. When considering the time to escape (Fig. 9), there was a significant difference found between the different barriers for both species of ant (ANOVA: *M. scabrinodis*, $F_{1,78}$=162.92, $P$<0.001; *P. dives*, $F_{1,64}$=13.076, $P$<0.001).

## DISCUSSION

### Trapping of ants by loose powders

For loose powder experiments, after placing the ants within the centre of the dish, workers were observed to pause and briefly investigate the barriers with their antennae before moving to another section or attempting to cross. Barriers constructed of the largest particles did not present a problem for the ants to either cross or escape from the dish after crossing. However, after crossing the powder barriers constructed of smaller particles, a loss of adhesion on the vertical smooth walls of the Petri dish was observed for both species of ant, with these adhesion failure events becoming more frequent with decreasing particle diameter. Several ants were observed to fall from the vertical glass wall back into the powder barrier after temporarily achieving adhesion to the glass.

Smaller particles were found to trap a significantly greater percentage of ants for both species, suggesting that contamination becomes a greater problem for locomotion the smaller the particles the insect encounters. For example, powder barriers constructed of the 1 μm diameter silica-glass particles and the 21 μm diameter PTFE

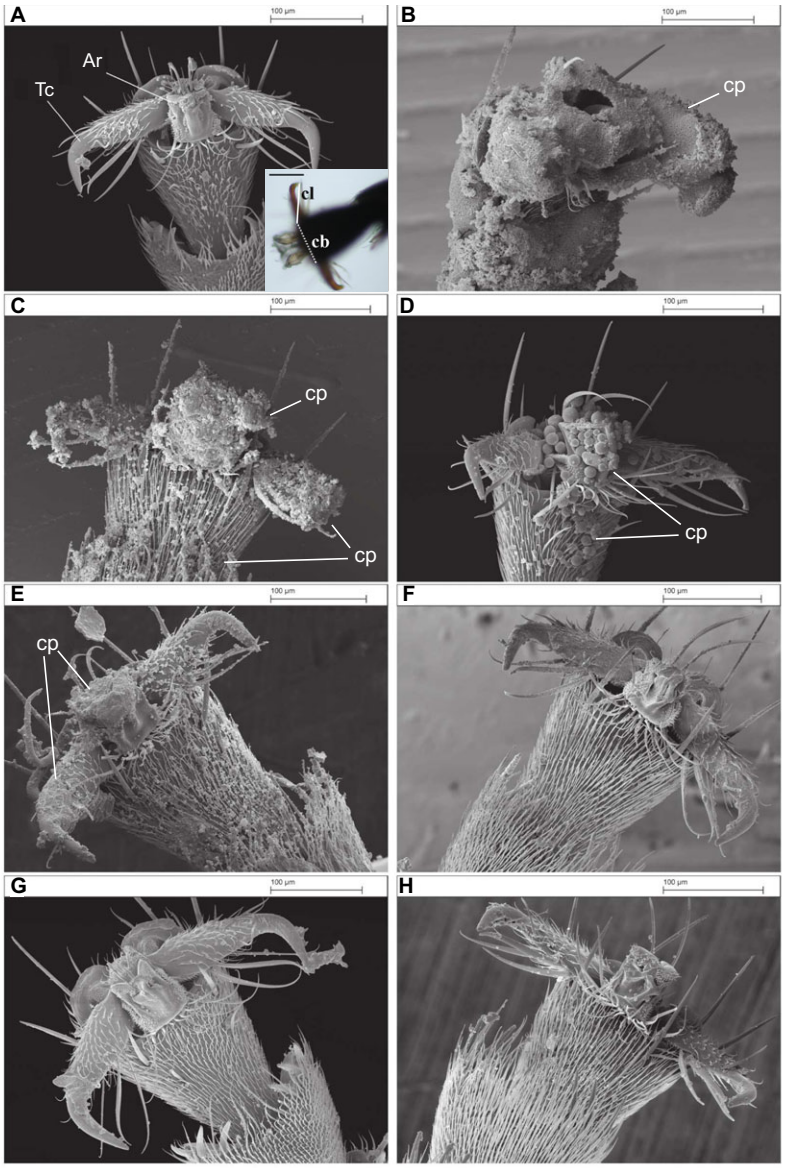


Fig. 4. SEM micrographs of *P. dives* tarsi (A) uncontaminated, and after traversing powder barriers constructed of glass (B,D,F,H) and PTFE (C,E,G); (B) 1 μm glass, (C) 21 μm PTFE, (D) 19 μm glass, (E) 105 μm PTFE, (F) 111 μm glass, (G) 123 μm PTFE and (H) 141 μm glass. The level of contamination decreases with increasing particle size, and is not strongly affected by material type. Larger particles of glass and PTFE were not found to adhere to the arolium, as evidenced by the lack of particles in F, G and H. Inset in A shows a dorsal view of a *P. dives* tarsus indicating how claw length (cl) and claw base (cb) were measured. Ar, arolium; cp, contaminating particles; Tc, tarsal claw. Scale bars, 100 μm.

particles each trapped over 90% of test insects for both species (Fig. 3).

The particle sizes found to heavily contaminate the arolium and tarsus of the ants corresponded well to those that also trapped greater than 50% of individual ants, with the exception of the 19 μm glass particles for *P. dives* (Fig. 3). This is reasonable because heavy contamination reduces the available contact area between arolium and substrate, which dramatically reduces adhesion and friction forces (Gorb and Gorb, 2002; Hosoda and Gorb, 2011). Our results therefore give further confirmation that the 'contamination hypothesis' (Gorb and Gorb, 2002) proposed for hairy pad systems, also applies to insects with smooth adhesive pads. Ants with contaminated arolia, however, displayed no obvious change in behaviour whilst walking on a horizontal surface, suggesting that arolia are not deployed to a significant extent in this case.

From Fig. 4 it can be seen that for both particle types when imaging with SEM, the arolia of ants that had traversed barriers made from the particles with diameters greater than approximately 100 μm were free from contamination or only lightly contaminated. One possible explanation for this observation is that when an ant crosses a powder barrier (consisting of multiple layers of particles), the relative magnitude of the competing forces between the pad and particles compared with inter-particle forces or particle weight may decrease with increasing particle size so that only particles below a certain threshold size will spontaneously adhere to the arolium. In the Appendix, we explore this possibility in detail through theoretical estimates of the different relevant forces. These estimates predict that only particles with a diameter greater than 4 mm will not adhere to the arolia. This is more than one order of magnitude larger than the threshold size observed in Fig. 4 and we therefore conclude that this is not the explanation for the observed threshold particle size.

We observed substantial contamination by large quantities of particles when particle diameters were smaller than the claw dimensions for both materials. For PTFE particles, heavy contamination was observed for particles with a mean diameter of 21 μm, light contamination was observed for 105 μm particles, and no contamination was observed for 123 μm particles. The light contamination by 105 μm diameter PTFE particles (Fig. 4E) appears to only consist of particulates of smaller size than the mean particle diameter. For glass, we observed heavy contamination by particles with mean diameters of 1 and 19 μm (Fig. 4B,D), and no

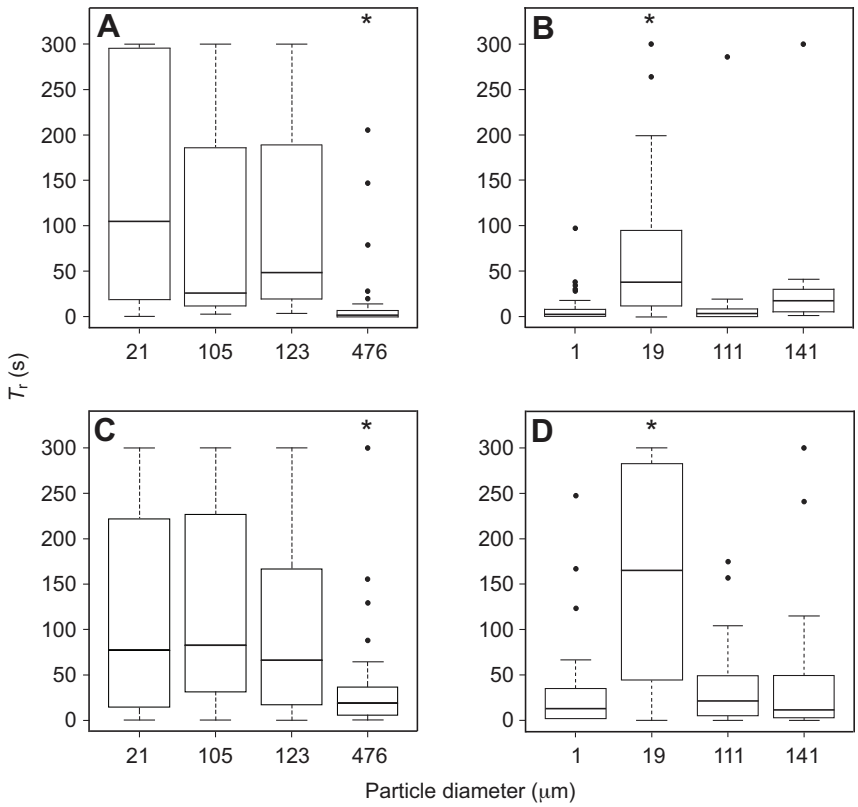


Fig. 5. Time taken by (A,B) *P. dives* and (C,D) *M. scabrinodis* to attempt to cross the threshold of the loose barriers, $T_r$, for different mean particle diameters of PTFE (A,C) and glass (B,D). Experiments were capped at 300 s (5 min). Plot shows medians (centre line), inter-quartile range (boxes) and the largest and smallest values (whiskers) that are not outliers (circles). Asterisks indicate median values that were significantly different from all other particle types: (A) ANOVA, $F_3$=7.47, 476 *vs* 21 μm $P$<0.001, 476 *vs* 105 μm $P$<0.05, 476 *vs* 123 μm $P$<0.01; (B) ANOVA, $F_3$=9.09, 19–1 μm $P$<0.001, 19–111 μm $P$<0.001, 19–141 μm $P$<0.05; (C) ANOVA, $F_3$=5.94, 476 *vs* 21 μm $P$<0.001, 476 *vs* 105 μm $P$<0.001, 476 *vs* 123 μm $P$<0.001; (D) ANOVA, $F_3$=22.00, 19 *vs* 1 μm $P$<0.01, 19 *vs* 111 μm $P$<0.001, 19 *vs* 141 μm $P$<0.05; all others were not significant.

contamination by particles with mean diameters of 111 and 141 μm (Fig. 4F,H). From Table 1 it can be seen that the standard deviation of the particle diameters for PTFE are relatively larger than those for glass, which suggests that only the smaller particles within a particular particle range adhere spontaneously – this may warrant further investigation.

We note that the transition from heavily contaminated arolia to non-contaminated arolia for *P. dives* (Fig. 4) occurs at a particle size comparable to the claw dimensions (Table 2). We propose that the size dependence for contamination may be explained by the fact that individual particles with diameter comparable to or greater than the claw dimensions are prevented from adhering to the arolium by the presence of the claws themselves during locomotion, whereas particles much smaller than the claw dimensions are able to make contact with and contaminate the most distal tarsal segment of the ant, including the arolium, in large numbers (Fig. 10). This leads to a reduction in real contact area with the substrate and a loss of adhesive force on subsequent steps, preventing the insect from scaling the vertical glass surface within the time limit. Thus we propose that, in ants, the claws may provide some protection from contaminants that are large relative to the claw dimensions becoming affixed to the adhesive pad or interfering with efficient arolium deployment. Presumably, this would also work towards reducing the amount of active grooming the insect may need to perform to keep the arolium functioning efficiently (Hosoda and Gorb, 2011).

It was found that a significantly lower percentage of ants were trapped by the 19 μm glass particle barriers than the 21 μm PTFE particles for both species of ant, even though the arolium and parts of the surrounding areas were contaminated in each case (Fig. 4). In order to understand this difference, we consider the behaviour of the ants after they had crossed the barrier threshold. After crossing the powder and approaching the vertical glass wall, the forelegs of the ants were observed to slide in a downward direction on the walls of the Petri dish in a scrambling, or shearing, motion as the ant attempted to gain adhesion to the surface. This behaviour was observed for both species, but *P. dives* were, in general, noticeably more active and would often spend a greater amount of time scrambling at the inner wall of the Petri dish attempting to escape. This behaviour occurred more frequently for smaller particles and often continued for some time, with the result that sufficient adhesion sometimes returned, and escape was achieved within the time limit for a number of ants. Additionally, after scrambling at the wall for some time, a number of ants would stop to groom their antennae and tarsi before continuing to attempt escape. This sequence of behaviours is similar to that found recently for the leaf beetle *Gastrophysa viridula* (Hosoda and Gorb, 2011), but included grooming of the antennae as well as the tarsus.

We suspect that contaminated tarsi of the ants could remove some adherent particles *via* the observed scrambling or shearing motion of the feet against the glass wall of the arena, in a behaviour akin to ‘self-cleaning’ in insects (Clemente et al., 2010), and geckos (Hansen and Autumn, 2005). However, this action will only be effective if (1) the downward pulling force exerted by the ant is large enough, and (2) the frictional force between the particle and the substrate is large enough to cause the particles attached to the pad to be dislodged during this shearing motion. We note that *P. dives* workers are on average stronger than *M. scabrinodis* owing to their larger size (Table 2). We also note that the friction coefficient of glass on glass is higher than for PTFE on glass (Lide, 2008). Thus, it is reasonable to assume that the observed scrambling motion should be most effective in removing the contaminating particles for *P. dives* contaminated by glass particles. This may explain why most of the *P. dives* workers (90.6%) were able to escape from the 19 μm glass powder barriers (Fig. 3) even though the arolium was clearly contaminated by these particles (Fig. 4), and would support the mechanism of self-cleaning in geckos proposed by Hansen and Autumn (Hansen and Autumn, 2005). It

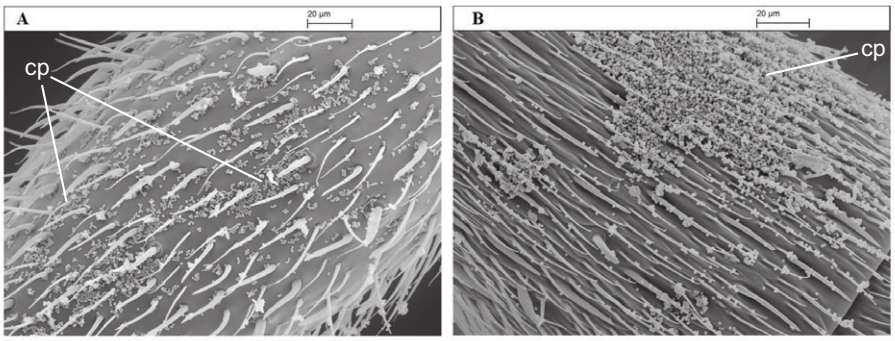


Fig. 6. SEM images of the terminal antenna segments (flagellomeres) of (A) *M. scabrinodis* and (B) *P. dives* contaminated with 1 µm glass particles. Scale bars, 20 µm.

was found (Clemente et al., 2010) that with a shearing motion, smooth adhesive pads are able to remove adherent particles after several steps. Individuals of *P. dives* in the present study took longer than this to regain sufficient adhesion in order to escape. This could be due to several factors: (1) the deposition of particles, and subsequent re-contamination of the arolium, from the glass surface as the ant attempted to escape from the same location of the dish; (2) a number of particles becoming embedded in the soft cuticle of the arolia within the contact zone; or (3) simply the sheer numbers of particles present in our case. As contamination and recovery time are strongly dependent upon contact area with the substrate, this continued presence of particles would slow the recovery process (Federle et al., 2002). This scrambling motion may work in a manner similar to that seen for hairy pads of insects (Clemente et al., 2010) and geckos (Hansen and Autumn, 2005); however, a detailed analysis of the mechanisms of the observed self-cleaning action in ants is beyond the scope of the current paper and is investigated in a separate publication (Orchard et al., 2012).

### Repellent effects of barriers

As reported above, ants were observed to investigate the barriers with their antennae before attempting to cross. Ants probed several sections of the barrier with their antennae in a manner similar to that reported for stick insects assessing gap sizes (Blaseing and Cruhe, 2004) and for cockroaches performing orientation behaviours (Camhi and Johnson, 1999; Okada and Toh, 2006), before either crossing or moving to another section. This behaviour was observed for barriers constructed of all particle diameters and materials. Ant workers of both species were observed to be repelled by the powders to some extent, but particularly so with the smaller particles. Because the ants studied here are not repelled by smooth, flat surfaces of either PTFE or glass (M.J.A. and M.J.O., personal observations), this suggests that it is the particulate nature of the materials that causes the ants to be repelled. However, the 1 µm glass particles were an exception to this observation, with the majority of ants spending less time investigating these barriers compared with the others (Fig. 5). Considering the low values of $T_r$ observed for ants crossing the 1 µm glass barriers (shown in Fig. 5), this may also be explained to some extent by the ants' behaviour. In many cases, ants presented with 1 µm glass barriers did not stop to investigate the powder and simply ran across the threshold, moving up to the glass wall without hesitation. In the remaining cases, the ants only investigated for a relatively short time, as evidenced by the low values of $T_r$ in Fig. 5. These observations suggest that the ants were either unable to detect the barriers or did not consider the barriers as something to be avoided.

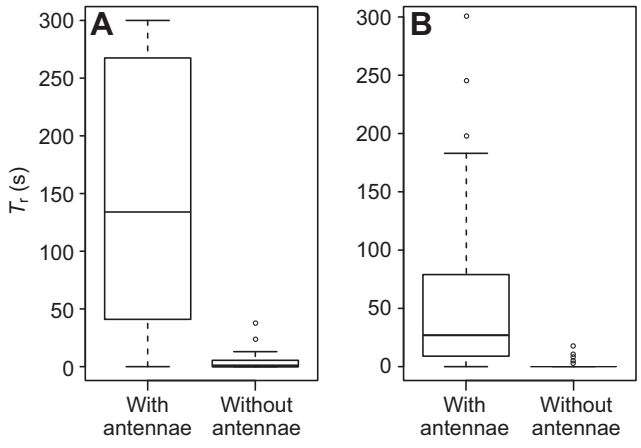


Fig. 7. Time repelled, $T_r$, for 19 µm glass particles for (A) *M. scabrinodis* and (B) *P. dives* with and without their antennae. There was a significant drop in time repelled for ants without antennae (*P. dives*, $F_1$=17.93, $P$<0.001; *M. scabrinodis*, $F_1$=31.538, $P$<0.001).

Often it was observed that after having touched the barriers with their antennae ants would spend time cleaning, or grooming, their antennae in a way similar to that described by Wheeler (Wheeler, 1907) and others (e.g. Farish, 1972). It has been found previously that hairs present on the antennae are involved in detection of various aspects of an ants' environment, including airflow, chemical signalling, as well as tactile sensing (Hölldobler and Wilson, 1990; Bernadou and Fourcassie, 2008; Benton, 2008). In the present case, these hairs may also be used to gain some degree of direct tactile feedback on the physical properties of their environment, such as mechanical fragility, which subsequently influences the ants' behaviour.

Contamination of the antenna's flagellomeres (sections) (shown in Fig. 6) may inhibit the insects' ability to accurately detect tactile cues such as mechanical fragility and make the 1 µm diameter powder barriers essentially invisible to the ants used in this study, with a combination of dense contamination of the adhesive pads, tarsi and antennae, along with the apparent inability to detect the individual particles making this barrier particularly effective at preventing insect locomotion on smooth surfaces. To investigate this hypothesis, we performed a series of barrier experiments with 19 µm glass particles using ants with and without antennae (Fig. 7). We found that ants without antennae spent significantly less time investigating the barriers before crossing than ants with antennae. The values for $T_r$ found in this case were similar to those found for ants crossing the 1 µm glass particles (Fig. 5), providing evidence to support this hypothesis.

### Rigid powder barriers

We note that for each species–material combination, the dependence of $T_r$ on particle diameter (Fig. 5) demonstrates a trend similar to

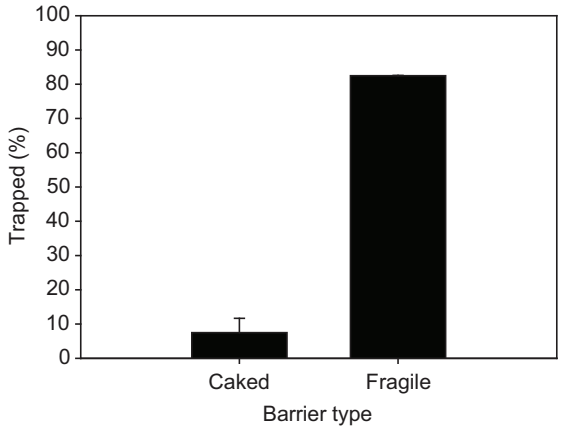


Fig. 8. Percentage of *M. scabrinodis* workers trapped by the loose ($N$=40) and caked ($N$=40) barriers constructed of the 19 μm glass particles. There was a significant decrease in the number of ants trapped by the caked barriers ($F_1$=102.6, $P$<0.001). Error bars show s.e.m.

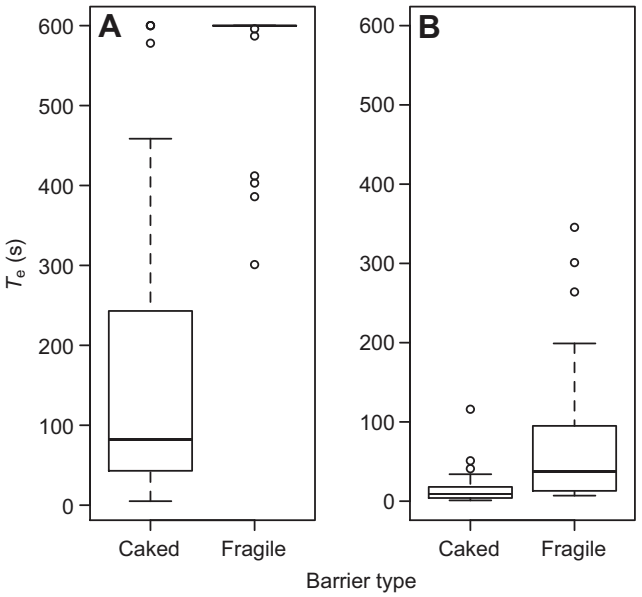


Fig. 9. Time to cross the powder barrier and escape, $T_e$, as a function of barrier type for (A) *M. scabrinodis* and (B) *P. dives*. $T_e$ was significantly different between caked and loose barriers (*P. dives*, $F_1$=13.07, $P$<0.001; *M. scabrinodis*, $F_1$=162, $P$<0.001).

the relationship between particle diameter and the percentage trapped (Fig. 3). This relationship suggests that repellence becomes more pronounced for particles that lead to a greater amount of contamination, which produces a significant reduction in adhesion *via* the reduction of the available contact area. The value $T_r$ measures the time taken by an insect to investigate the barriers with their antennae before crossing, and as such is not determined by arolia contamination. Instead, the correlation of $T_r$ with the percentage of ants trapped suggests that the ants are able to gather information about the barriers *via* the observed antennating action.

To determine whether the observed repellence was principally due to the barriers' particulate nature, escape experiments with both caked and fragile barriers were repeated. After placing the ants inside the circular barriers, it was obvious that the caked barriers were significantly easier to traverse and caused very little difficulty for the ants to subsequently climb the smooth glass wall of the dish and escape. A significantly lower percentage of *M. scabrinodis* were trapped by the caked barriers, and a significant drop in $T_e$ suggests that individuals of this species were not repelled by these rigid and rough surfaces. For *P. dives*, there was no significant difference found between the barrier types because all individuals of this species were able to escape. However, those *P. dives* workers that did escape took a significantly longer time to do so, as shown in Fig. 9. Because the barriers differ only in their fragility, these results provide evidence to support the suggestion (see the previous section) that the fragile nature of the powder barriers is crucial to their effectiveness at trapping ants *via* contamination of the adhesive pads, in much the same way that plant epicuticular wax blooms function (Stork, 1980b; Gorb et al., 2008; Borodich et al., 2010), and that ants may assess the contamination risk of the powders by using their antennae to probe the mechanical fragility of the barriers.

## Conclusions

We studied the escape of two different ant species (*P. dives* and *M. scabrinodis*) from circular powder barriers in order to determine the effect of barrier properties such as particle size, surface energy and mechanical fragility and environmental factors such as humidity on insect adhesion and repellence. Our results demonstrate that the anti-adhesive effect of barriers, constructed from loose synthetic powders, is due to contamination of the insects' attachment devices causing a reduced contact area between the adhesive pad and the adherent surface, and was independent of RH within the range tested. Adhesive loss is due principally to this loss of contact area between the substrate and the adhesive pad, preventing adhesion to smooth surfaces for some time after contamination. Our results therefore show that the 'contamination hypothesis', proposed previously (Gorb and Gorb, 2002) for hairy pad systems, also applies to insects with smooth adhesive pads.

We found that contamination of the adhesive arolia, and the proportion of ants trapped by loose powder barriers, is strongly dependent on the size of the individual particles, but is less significantly dependent on particle surface energy and not dependent on environmental factors such as relative humidity. Specifically, particles larger than the tarsal claw base distance did not contaminate the arolia of either ant species, whereas particles smaller than the claw dimensions did, often in great numbers. This suggests that the claws may offer the arolium some protection from being contaminated by particles that are large relative to the claw dimensions. Workers of *P. dives* contaminated with high-energy particles regain adhesion after time spent scrambling at a high-energy smooth substrate in a shearing motion, similar to that seen in geckos and other insects in previous studies. This action may be a further example of 'self-cleaning' in smooth pads (Orchard et al., 2012).

We also found evidence that ants used in this study were repelled by the loose powders, particularly by barriers made from the smaller particles, which lead to a greater amount of arolia contamination and loss of adhesion, with the exception of 1 μm particles. Repellence by a given powder barrier was significantly reduced when the mechanical rigidity of the barrier was increased. These results suggest that ants may be able to use their antennae to probe the mechanical fragility of the barriers and, furthermore, use this information to alter their behaviour in order to minimise the risk of contamination to their arolia. The ants' ability to probe vital

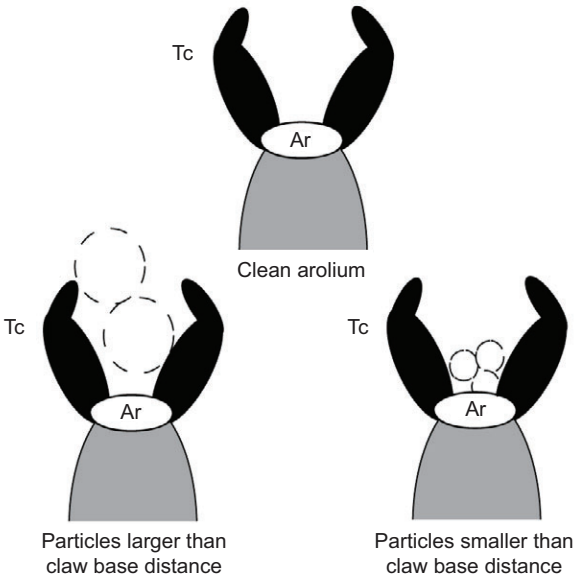


Fig. 10. Schematic of a ventral view of the distal tarsomere of an ant tarsus showing the arolium (Ar) and tarsal claws (Tc). A possible mechanism by which the tarsal claws may prevent large particles from attaching to the partially exposed arolium is shown. Particles with diameters greater than the claw dimensions are prevented from making contact with the soft adhesive pad.

physical properties of its environment using its antennae will be the subject of a detailed investigation in the near future.

Our results show that similar effects of contamination of adhesive pads in ants can occur for both natural (plant waxes) and synthetic particles. Results of this study show some agreement with data published for particulate control of insect pests (Briscoe, 1943; Alexander et al., 1944; Merton, 1956, Boiteau et al., 1994; Glenn et al., 1999; Puterka et al., 2000; Hunt and Vernon, 2001) and suggest that the results presented in these studies are likely a result of the small particle sizes used. Mimicking the effect of natural barriers could lead to the production of more efficient synthetic and non-toxic means of controlling pest species in agriculture, as well as for domestic purposes.

## APPENDIX

In this Appendix we estimate the pad–particle force and the inter-particle forces, or particle weight, for an ant crossing a powder barrier (which consists of multiple particle layers) to estimate how the relative magnitude of these competing forces varies with particle diameter. We make the plausible assumption that contamination of the arolium will only occur when the particle–arolium force exceeds both the particle–particle force and the force due to the particle weight. This then allows us to make a theoretical estimate of the threshold diameter below which particle contamination of the arolium should occur, in an approach similar to that of Hansen and Autumn (Hansen and Autumn, 2005).

### Particle–arolium force

To estimate the particle–arolium force, we assume that the particle is rigid whereas the arolia is a soft elastic material with Young's modulus $E$ and Poisson ratio $\nu$ that is covered by a uniform thin film of adhesive secretion of thickness $h$. Assuming that the particle–arolium force arises from capillary forces due to the adhesive secretion and that the secretion perfectly wets the arolia and both the particle types, the attractive force between the particle and arolia ($F_{pa}$) is given by (Butt et al., 2010):

$$F_{pa} = 4\pi\gamma R + \left(\frac{\pi\gamma}{2r}\right)^3 \frac{2R^2}{3E^{*2}}\ , \tag{A1}$$

with:

$$E^* = \frac{E}{1-\nu^2}\ . \tag{A2}$$

Here, $\gamma$ is the surface tension of the secretion, $R$ is the radius of the particle asperity in contact with the arolium, $r$ is the radius of curvature of the meniscus formed by the thin film of adhesive secretion wicking up around the particle asperity, and $E^*$ is the effective elastic modulus. For spherical particles, such as the glass particles used in this study, $R$ is equal to the radius of the particle, whereas for irregularly shaped particles, such as the PTFE particles used in this study, $R$ is less than the mean radius of the particle. In contrast, the radius of curvature of the meniscus $r$ arises from a balance of the capillary pressure of the meniscus and disjoining pressure of the thin liquid film (Mate, 2008).

The first term on the right-hand side of Eqn A1 represents the capillary force between a rigid particle and a rigid flat substrate (Mate, 2008) whereas the second term is the additional contribution to the capillary force arising from the deformation of the soft elastic substrate (Butt et al., 2010). For soft substrates with small menisci of radii $r$, the second term can be significant. However, its exact magnitude is difficult to estimate because it contains a number of parameters such as $E$, $\nu$ and $r$ that are difficult to measure and are therefore not accurately known for the system at hand. Fortunately, for the purposes of estimating a threshold diameter, it is sufficient to approximate the particle–arolia force using the first term only, i.e.:

$$F_{pa} \approx 4\pi\gamma R\,. \tag{A3}$$

This represents a lower bound for the adhesive force. Having predicted a threshold diameter, we will then include the second term to see what qualitative effect it has on the predicted value.

### Particle–particle force

Capillary forces between particles within the barrier were assumed to be negligible below relative humidities of 95% because of the small value of the Kelvin radius below this point. For example, it has been shown (Kohonen and Christenson, 2000) that the mean radius of curvature of capillary condensates between rinsed mica surfaces is <10 nm for relative humidities below 96%. Particle–particle forces ($F_{pp}$) are thus primarily due to van der Waals attractive forces (Duncan et al., 2007), which are given by Israelachvili (Israelachvili, 2007) and Mate (Mate, 2008) as:

$$F_{pp} = \frac{AR}{12D^2}\ , \tag{A4}$$

where $R$ is the radius of the two asperities in contact with each other (assumed to be equal), $A$ is the particle–air–particle Hamaker constant and $D$ is the distance of closest approach between the two asperities.

### Particle weight

The weight of a particle ($F_w$) is given by:

$$F_w = \frac{4\pi}{3} R_p^3 g\rho\ , \tag{A5}$$

where ρ is the density of the particle material, $\boldsymbol{g}$ is the acceleration due to gravity and $R_p$ is here defined as the (mean) radius of the particle rather than the asperity radius.

### Relative magnitude of forces

We first compare the relative magnitude of particle–arolium and particle–particle forces. From Eqns A3 and A4, this is given by:

$$\frac{F_{pp}}{F_{pa}} = \frac{A}{48\pi\gamma D^2} \ . \quad \text{(A6)}$$

We note that the ratio above is independent of asperity radius $R$. For γ, we use the literature estimate of $\gamma \approx 30\,\text{mN}\,\text{m}^{-1}$ (Federle et al., 2002). The Hamaker constant for glass particle–air–glass particle is given by $A_{\text{glass-air-glass}} \approx 6\times10^{-20}\,\text{J}$ whereas the Hamaker constant for PTFE particle–air–PTFE particle is $A_{\text{PTFE-air-PTFE}} \approx 4\times10^{-20}\,\text{J}$ (Israelachvili, 2007). Finally, we estimate the minimum separation distance $D$ to be ~10 nm based on the nano-roughness of the asperities making contact.

Using these parameters, we find $F_{pp}/F_{pa}=1.3\times10^{-4}$ in the case of glass particles and PTFE particles on glass, and $F_{pp}=F_{pa}=8.8\times10^{-5}$ in the case of PTFE particles. This shows that that the capillary forces acting between the arolium and the particles is always approximately four orders of magnitude greater than the van der Waals attractive forces between the particles within the barrier, independent of $R$. If we include the substrate deformation contribution to the particle–arolium force (i.e. Eqn A1), this will lead to an even greater discrepancy between the particle–arolium force and the particle–particle forces.

We next compare the relative magnitude of the particle–arolium force with the weight of the particle. From Eqns A3 and A5, this is given by:

$$\frac{F_w/F_{pa}}{F_{pa}} = \frac{3\gamma}{R_p^2\rho g} \ . \quad \text{(A7)}$$

For the irregular PTFE particles, making this assumption leads to an overestimate of the particle–arolium force. However, we believe that this approximation is adequate as we are only interested in making order-of-magnitude estimates of the different forces here.

When the above ratio is equal to unity, the weight of the particle is comparable to the adhesive force generated by the capillary force between the arolium and the particle. This occurs for the threshold radius, $R_c$:

$$R_c = \sqrt{\frac{3\gamma}{\rho g}} \ , \quad \text{(A8)}$$

i.e. the particle–arolium force exceeds the particle weight only for $R_P<R_c$. Using $\rho=2000\,\text{kg}\,\text{m}^{-3}$ for PTFE and $\rho=2350\,\text{kg}\,\text{m}^{-3}$ for the glass particles, we find $R_c \approx 2$ mm for both PTFE and glass particles, i.e. a threshold diameter of approximately 4 mm. This value is over one order of magnitude larger than the threshold size of 100 μm observed experimentally for both PTFE and glass particles (Fig. 4). Including the substrate deformation contribution to the particle–arolium force will lead to an even higher value for the threshold diameter. We therefore conclude that the threshold particle size for contamination is not determined by a competition between the particle–arolium forces and either particle–particle or gravitational forces.

### LIST OF SYMBOLS AND ABBREVIATIONS

| | |
|---|---|
| $A$ | Hamaker constant |
| $D$ | closest approach distance of two surface asperities |
| $E^*$ | effective elastic modulus |
| $E$ | bulk elastic modulus |
| $F_{pa}$ | force between particle and arolium |
| $F_{pp}$ | force between two adherent particles |
| $F_w$ | force due to particle weight |
| $\boldsymbol{g}$ | acceleration due to gravity |
| $h_{ant}$ | height of ant |
| $h_d$ | height of Petri dish |
| $N_e$ | number of ants escaped |
| $N_n$ | number of ants making no attempt to escape |
| $N_t$ | number of ants trapped |
| $N_{total}$ | total number of ants tested within a single species |
| $r$ | radius of curvature of liquid meniscus |
| $R$ | radius of particle asperity |
| $R_c$ | contamination threshold particle radius |
| $r_d$ | radius of Petri dish |
| RH | relative humidity |
| $R_p$ | mean particle radius |
| γ | liquid surface tension |
| ν | Poisson ratio |
| ρ | material density |


### ACKNOWLEDGEMENTS

The authors would like to thank Mr Tony Sinclair at the Department of Biological Sciences, University of Hull, for his tireless efforts in the SEM suite, along with two anonymous reviewers for very helpful comments on the original manuscript.

### FUNDING

M.J.A. and M.J.O. thank the University of Hull, UK, for financial support in the form of two University of Hull 80th Anniversary PhD Scholarships.


### REFERENCES


**Alexander, P., Kitchener, J. and Briscoe, H**. (1944). Inert dust insecticides. *Ann. Appl. Biol.* **31**, 143-159.

**Bauer, U., Bohn, H. and Federle, W.** (2008). Harmless nectar source or deadly trap: *Nepenthes* pitchers are activated by rain, condensation and nectar. *Proc. R. Soc. Lond. B* **275**, 259-265.

**Benton, R.** (2008). Chemical signalling in *Drosophila. Curr. Opin. Neurobiol.* 18, 357-363.

**Bernadou, A. and Fourcassie, V.** (2008). Does substrate coarseness matter for foraging ants? An experiment with *Lasius niger* (Hymenoptera; Formicidae). *J. Insect Physiol.* **54**, 534-542.

**Bernadou, A., Démares, F., Couret-Fauvel, T., Sandoz, J. and Gauthier, M.** (2009). Effect of fipronil on side-specific antennal tactile learning in the honeybee. *J. Insect Physiol.* **55**, 1099-1106.

**Betz, O. and Kolsch, G.** (2004). The role of adhesion in prey capture and predator defence in arthropods. *Arthropod Struct. Dev.* **33**, 3-30.

**Bitar, L., Voigt, D., Zebitz, C. and Gorb, S. N** (2009). Tarsal morphology and attachment ability of the codling moth *Cydia pomonella* L. (Lepidoptera, Tortricidae) to smooth surfaces. *J. Insect Physiol.* **55**, 1029-1038.

**Bitar, L., Voigt, D., Zebitz, C. and Gorb, S. N.** (2010). Attachment ability of the codling moth *Cydia pomonella* L. to rough substrates. *J. Insect Physiol.* **56**, 1966-1972.

**Blaseing, B. and Cruhe, H.** (2004). Stick insect locomotion in a complex environment: climbing over large gaps. *J. Exp. Biol.* **207**, 1273-1286.

**Bocquet, L., Charlaix, E., Cilberto, S. and Crassous, J.** (1998). Moisture-induced ageing in granular media and the kinetics of capillary condensation. *Nature* **396**, 735-737.

**Bocquet, L., Charlaix, E. and Restagno, F.** (2002). Physics of humid granular media. *C. R. Phys.* **3**, 207-215.

**Boiteau, G., Pelletier, Y., Misener, G. C. and Bernard, G.** (1994). Development and evaluation of a plastic trench barrier for protection of potato from walking adult Colorado potato beetles (Coleoptera: Chrysomelidae). *J. Econ. Entomol.* **87**, 1325-1331.

**Borodich, F., Gorb, E. V. and Gorb, S. N.** (2010). Fracture behaviour of plant epicuticular wax crystals and its role in preventing insect attachment: a theoretical approach. *Appl. Phys. A* **100**, 63-71.

**Briscoe, H.** (1943). Some new properties of inorganic dusts. *J. R. Soc. Arts* **91**, 593-607.

**Butt, H., Barnes, W., del Campo, A., Kappl, M. and Schönfeld, F.** (2010). Capillary forces between soft, elastic spheres. *Soft Matter* **6**, 5930-5963.

**Camhi, J. and Johnson, E.** (1999). High-frequency steering maneuvers mediated by tactile cues: antennal wall-following in the cockroach. *J. Exp. Biol.* **202**, 631-643.

**Clemente, C., Bullock, J., Beale, A. and Federle, W.** (2010). Evidence for self-cleaning in fluid based smooth and hairy adhesive systems of insects. *J. Exp. Biol.* **213**, 635-642.

**Crook, D. J., Kerr, L. M. and Mastro, V. C.** (2008). Sensilla on the antennal flagellum of *Sirex noctilio* (Hymenoptera: Siricidae). *Ann. Entomol. Soc. Am.* **101**, 1094-1102.

**Dirks, J.-H., Clemente, C. and Federle, W.** (2009). Insect tricks: two phasic foot pad secretion prevents slipping. *J. R. Soc. Interface* **7**, 587-593.

**Dixon, A., Croghan, P. and Gowing, R.** (1990). The mechanism by which aphids adhere to smooth surfaces. *J. Exp. Biol.* **152**, 243-253.

**Drechsler, P. and Federle, W.** (2006). Biomechanics of smooth adhesive pads in insects: influence of tarsal secretion on attachment performance. *J. Comp. Physiol. A* **192**, 1213-1222.
**Duncan, R. P., Autumn K. and Binford, G. J.** (2007). Convergent setal morphology in sand-covering spiders suggests a design principle for particle capture. *Proc. R. Soc. Lond. B* **274**, 3049-3056.
**Eigenbrode, S.** (2004). The effects of plant epicuticular waxy blooms on attachment and effectiveness of predatory insects. *Arthropod Struct. Dev.* **33**, 91-102.
**Eisner, T. and Aneshansley, D.** (2000). Defense by foot adhesion in a beetle (*Hemisphaerota cyanea*). *Proc. Natl. Acad. Sci. USA* **97**, 6568-6573.
**Farish, D.** (1972). The evolutionary implications of qualitative variation in the grooming behaviour of the Hymenoptera (Insecta). *Anim. Behav.* **20**, 662-676.
**Federle, W., Maschwitz, U., Fiala, B., Riederer, M. and Hölldobler, B.** (1997). Slippery ant-plants and skilful climbers: selection and protection of specific ant partners by epicuticular wax blooms in *Macaranga* (Euphorbiaceae). *Oecologia* **112**, 217-224.
**Federle, W., Rohrseitz, K. and Hölldobler, B.** (2000). Attachment forces of ants measured with a centrifuge: better 'wax-runners' have a poorer attachment to a smooth surface. *J. Exp. Biol.* **203**, 505-512.
**Federle, W., Riehle, M., Curtis, A. and Full, R.** (2002). An integrative study of insect adhesion: mechanics and wet adhesion of pretarsal pads in ants. *Integr. Comp. Biol.* **42**, 1100-1106.
**Fraysse, N., Thomé, H. and Petit, L.** (1999). Humidity effects on the stability of a sandpile. *Eur. Phys. J. B* **11**, 615-619.
**Gaume, L., Perret, P., Gorb, E. V., Gorb, S. N., Labat, J.-J. and Rowe, N.** (2004). How do plant waxes cause flies to slide? Experimental tests of wax-based trapping mechanisms in three pitfall carnivorous plants. *Arthropod Struct. Dev.* **33**, 103-111.
**Gladun, D., Gorb, S. N. and Frantsevich, L.** (2009). Alternative tasks of the insect arolium with special reference to Hymenoptera. In *Functional Surfaces in Biology – Adhesion Related Phenomena*, Vol. 2 (ed. S. Gorb), pp. 67-103. London: Springer.
**Glenn, D., Puterka, G., Vanderzwet, T., Byers, R. and Feldhake, C.** (1999). Hydrophobic particle films: a new paradigm for suppression of arthropod pests and plant diseases. *J. Econ. Entomol.* **92**, 759-771.
**Gorb, E. V. and Gorb, S. N.** (2002). Attachment ability of the beetle *Chrysolina fastuosa* on various plant surfaces. *Entomol. Exp. Appl.* **105**, 13-28.
**Gorb, E. V. and Gorb, S. N.** (2009). Effects of surface topography and chemistry of *Rumex obtusifolius* leaves on the attachment of the beetle *Gastrophysa viridula*. *Entomol. Exp. Appl.* **130**, 222-228.
**Gorb, E. V., Voigt, D., Eigenbrode, S. D. and Gorb, S. N.** (2008). Attachment force of the beetle *Cryptolaemus montrouzieri* (Coleoptera: Coccinellidae) on leaflet surfaces of mutants of the pea *Pisum sativum* (Fabaceae) with regular and reduced wax coverage. *Arthropod Plant Interact.* **2**, 247-259.
**Gorb, S. N.** (1998). The design of the fly adhesive pad: distal tenent setae are adapted to the delivery of an adhesive secretion. *Proc. R. Soc. Lond. B* **265**, 747-752.
**Gorb, S. N. and Beutel, R. G.** (2001). Evolution of locomotory attachment pads of hexapods. *Naturwissenschaften* **88**, 530-534.
**Hansen, W. and Autumn, K.** (2005). Evidence for self-cleaning in gecko setae. *Proc. Natl. Acad. Sci. USA* **102**, 358-389.
**Hölldobler, B. and Wilson, E.** (1990). *The Ants*. Cambridge, MA: Belknap Press of Harvard University Press.
**Hosoda, N. and Gorb, S. N** (2011). Friction force reduction triggers feet grooming behaviour in beetles. *Proc. R. Soc. Lond. B* **278**, 1748-1752.
**Hunt, D. and Vernon, R.** (2001). Portable trench barrier for protecting edges of tomato fields from Colorado potato beetles (Coleoptera: Chrysomelidae). *J. Econ. Entomol.* **94**, 204-207.
**Ishii, S.** (1987). Adhesion of a leaf feeding ladybird *Epilachna vigintioctomaculta* (Coleoptera: Coccinellidae) on a vertically smooth surface. *Appl. Entomol. Zool.* **22**, 222-228.
**Israelachvili, J.** (2007). *Intermolecular and Surface Forces*, 2nd edn. London: Academic Press.
**Kevan, P. and Lane, M.** (1985). Flower petal microtexture is a tactile cue for bees. *Proc. Natl. Acad. Sci. USA* **82**, 4750-4752.
**Kohonen, M. and Christenson, H.** (2000). Capillary condensation of water between rinsed mica surfaces. *Langmuir* **16**, 7285-7288.
**Lee, J. and Fearing, R. S.** (2008). Contact self-cleaning of synthetic gecko adhesive from polymer microfibres. *Langmuir* **24**, 10587-10591.
**Lees, A. and Hardie, J.** (1988). The organs of adhesion in the aphid *Megoura viciae*. *J. Exp. Biol.* **136**, 209-228.
**Lide, D. R.** (2008). *CRC Handbook of Chemistry and Physics*, 88th edn (CD-ROM Version 2008). Boca Raton, FL: CRC Press/Taylor and Francis.
**Loeffler, H.** (2009). *Ant Adhesion and its Implications for Ant Behaviour*. MSc thesis, University of Hull, UK.
**Markstädter, C., Federle,W., Jetter, R., Riederer, M. and Hölldobler, B.** (2000). Chemical composition of the slippery epicuticular wax blooms on *Macaranga* (Euphorbiaceae) ant-plants. *Chemoecology* **10**, 33-40.
**Mate, C. M.** (2008). *Tribology on the Small Scale – A Bottom Up Approach to Friction, Lubrication and Wear*. New York: Oxford University Press.
**Merton, T.** (1956). On a barrier against insects. *Proc. R. Soc. Lond. A* **234**, 218-220.
**Nachtigall, W.** (1974). *Biological Mechanisms of Attachment: The Comparative Morphology and Bioengineering of Organs for Linkage, Suction, and Adhesion*. Berlin, Heidelberg, New York: Springer-Verlag.
**Okada, J. and Toh, Y.** (2006). Active tactile sensing for localization of objects by the cockroach antenna. *J. Comp. Physiol. A* **192**, 715-726.
**Orchard, M. J., Kohonen, M. and Humphries, S.** (2012). The influence of surface energy on the self-cleaning of insect adhesive devices. *J. Exp. Biol.* **215**, 279-286.
**Puterka, G., Glenn, D., Sekutowski, D., Unruh, T. and Jones, S.** (2000). Progress towards liquid formulations of particle films for insect and disease control in pear. *Environ. Entomol.* **29**, 329-339.
**R Core Development Team** (2010). *R: A Language and Environment for Statistical Computing*. Vienna, Austria: R Foundation for Statistical Computing, Vienna, Austria.
**Rasband, W.** (1997–2009). ImageJ 1.40. http://rsb.info.nih.gov/ij/.
**Stork, N.** (1980a). Experimental analysis of adhesion of *Chrysolina polita* (Chrysomelidae: Coleoptera) on a variety of surfaces. *J. Exp. Biol.* **88**, 91-107.
**Stork, N.** (1980b). Role of waxblooms in preventing attachment to brassicas by the mustard beetle, *Phaedon cochleariae*. *Entomol. Exp. Appl.* **28**, 100-107.
**Voigt, D., Schuppert, J. M., Dattinger, S. and Gorb, S. N.** (2010). Temporary stay at various environmental humidities affects attachment ability of Colorado potato beetles *Leptinotarsa decemlineata* (Coleoptera, Chrysomelidae). *J. Zool.* **281**, 227-231.
**Vötsch, W., Nicholson, G., Muller, R., Stierhof, Y.-D., Gorb, S. N. and Schwarz, U.** (2002). Chemical composition of the attachment pad secretion of the locust (*Locusta migratoria*). *Insect Biochem. Mol. Biol.* **32**, 1605-1613.
**Walker, G.** (1993). Adhesion to smooth surfaces by insects – a review. *Int. J. Adhes. Adhes.* **13**, 3-7.
**Walker, G., Yulf, A. and Ratcliffe, J.** (1985). The adhesive organ of the blowfly, *Calliphora vomitoria*: a functional approach (Diptera: Calliphoridae). *J. Zool.* **205**, 297-307.
**Wheeler, W.** (1907). On certain modified hairs peculiar to the ants of arid regions. *Biol. Bull.* **13**, 185-202.
**Wigglesworth, V.** (1987). How does a fly cling to the under surface of a glass sheet? *J. Exp. Biol.* **129**, 373-376.